Geomechanics and Engineering, *Vol. 6, No. 6 (2014) 531-544*
DOI: http://dx.doi.org/10.12989/gae.2014.6.6.531

Seismic response analysis of layered soils considering effect of surcharge mass using HFTD approach. Part II: Nonlinear HFTD and numerical examples

Mohammad A. Saffarian * and Mohammad H. Bagheripour [a]

Department of Civil Engineering, Shahid Bahonar University of Kerman, P.O. BOX 76165, Iran

(*Received June 19, 2013, Revised December 26, 2013, Accepted January 11, 2014*)

Abstract. Studies of earthquakes over the last 50 years and the examination of dynamic soil behavior reveal that soil behavior is highly nonlinear and hysteretic even at small strains. Nonlinear behavior of soils during a seismic event has a predominant role in current site response analysis approaches. Common approaches to ground response analysis include linear, equivalent linear and nonlinear methods. These methods of ground response analysis may also be categorized into time domain and frequency domain concepts. Simplicity in developing analytical relations and accuracy in considering soils' dynamic properties dependency to loading frequency are benefits of frequency domain analysis. On the other hand, nonlinear methods are complicated and time consuming mainly because of their step by step integrations in time intervals. In part I of this paper, governing equations for seismic response analysis of surcharged and layered soils were developed using fundamental of wave propagation theory based on transfer function and boundary conditions. In this part, nonlinear seismic ground response is analyzed using extended HFTD method. The extended HFTD method benefits Newton-Raphson procedure which applies regular iterations and follows soils' fundamental stress-strain curve until convergence is achieved. The nonlinear HFTD approach developed here are applied to some examples presented in this part of the paper. Case studies are carried in which effects of some influencing parameters on the response are investigated. Results show that the current approach is sufficiently accurate, efficient, and fast converging. Discussions on the results obtained are presented throughout this part of the paper.

Keywords: nonlinear analysis; ground response; surcharge mass; layered soils; HFTD approach

1. Introduction

The method of HFTD is, in fact, a procedure that takes the advantage of both time domain and frequency domain methods to optimize the solution particularly for nonlinear problem (Wolf 1986, Darber and Wolf 1988). In summary, by HFTD method, the equation of motion is solved in frequency domain and the nonlinearities are accounted for by time domain analysis. Latest development in HFTD approach are found in works conducted by Bazrafshan Moghaddam and Bagheripour (2012a, b). HFTD method can be conducted by various approaches which are summarized in these references. Bazrafshan Moghaddam and Bagheripour (2012a) presented

*Corresponding author, Master, E-mail: amin.safarian@yahoo.com
[a] Associate Professor, E-mail: bagheri@uk.ac.ir

http://www.techno-press.org/?journal=gae&subpage=7 ISSN: 2005-307X (Print), 2092-6219 (Online)

formulation of a Hybrid Frequency Time Domain (HFTD) method for the solution of nonlinear ground response problem using a non-recursive matrix approach. Time-frequency analysis of seismic ground response was presented also by Bazrafshan and Bagheripour (2012b) using a new compatible wavelet function family. The method was advantageous over other approaches since wavelets replaced the Fourier Transforms. Each earthquake record was low-pass filtered using a multi-resolution decomposition technique which provided a clear time-frequency view of earthquake signal. Based on the seismological approaches for processing recorded data, Zerva *et al*. (2012) presented a framework for simulation of ground motion particularly for acceleration time histories. They established the corner frequency of the high-pass filter by minimizing the effect of processing on the structural response that was used for response evaluation of which the ground motions were generated. They proposed two-step criterion which selected the filter corner frequencies by considering both the dynamic and the pseudo-static response of the system. Anbazhagan *et al*. (2011) examined the efficiency and applicability of available amplification relations in the literature for shallow engineering bedrock sites and carried site response studies using shear wave velocity of 13 sites selected for their studies. They used and compared empirical relations for amplification of seismic waves which were dependent on the ratio of shear wave velocity. Roy and Sahu (2012) conducted a study on spatial variation of ground motion in Kolkata metropolitan area using systematically generated ground motion considering the point source model coupled with site response analysis. Acceleration time histories at 121 boreholes for the vulnerable source due to maximum credible earthquake (MCE) were synthetically generated. Surface ground level motion parameters were determined using SHAKE 2000 software. Results presented in terms of PGA at borehole and surface, amplification factor, and surface response spectrum. Jayaram *et al*. (2011) conducted a study on the spectral acceleration correlation from Japanese earthquake ground motion data including data from both crustal and subduction zone earthquakes. The effect of ground motion model, earthquake source mechanism, seismic zone, site condition, and source to site distance on estimated correlations was evaluated and discussed. Some differences in correlations between earthquake source zones and earthquake mechanism were observed and tables of correlations coefficients for each specific case were provided.

Seismic response of a 3-stoty R-C structure resting on soft soil during Lefkada strong earthquake of 14/8/2003 was investigated by Giarlelis *et al.* (2011). The unusually strong levels of ground motion with PGA = 0.48 and Sa_{max} = 2.2 g recorded at approximately 10 km from causative fault had surprisingly low structural damages. Structural, geotechnical, and seismological aspect of earthquake were discussed. Detailed spectral and time history analysis highlighted the interplay of soil, foundation, and superstructure in modifying seismic demand in two orthogonal dimensions of the bulding.

Commonly, FFT and IFFT are used for the transformation of the results from one domain to the other and vice versa. A regular iteration scheme based on the variation of stiffness and damping in soil material is rationally followed on the soil's stress-strain curve until the convergence is reached. In the present part of paper, software has been developed using MATLAB code of practice for ground response analysis based on HFTD. An advantage of the method is the capability of nonlinear analysis of multilayer soil system having diverse material characteristics as well as the possibility of existing surcharge mass on ground surface.

2. Nonlinear HFTD method and mathematical formulation

A layered soil system including *m* layers overlain the bedrock is considered. The bedrock itself

is denoted as $m + 1^{th}$ layer and is subjected to a seismic excitation for which the time history of the strong motion is available. Concise review and the main steps in an HFTD procedure developed here are described in the following. These steps are, in fact, similar but extended version of the method developed and discussed earlier by Asgari and Bagheripour (2010).

Step 1: Performing FFT on the discrete values of the strong motion record, the frequency domain input at the bedrock is established.

$$u_{m+1}(\omega) = FFT(u_{m+1}(t)) = \sum_{\omega=1}^{N} u_{m+1}(t) w_N^{(\omega-1)(t-1)}, w_N = e^{-2\pi i/N}, i = \sqrt{-1} \tag{1}$$

In which ω is the loading frequency and N is the number of discrete acceleration values**.** u_n is the displacement at the top of n^{th} layer.

Step 2: The solution of the equation of motion considering surcharge mass based on the 1-D theory of the wave propagation in visco-elastic media is used to calculate the amplitudes of the steady state harmonic waves traveling up and down in the soil layers denoted by E_{n+1} and F_{n+1}

$$E_{n+1} = \frac{1}{2}\left[E_n(1+\alpha_n^*)e^{ik_n^* h_n} + F_n(1-\alpha_n^*)e^{-ik_n^* h_n}\right] \tag{2}$$

$$F_{n+1} = \frac{1}{2}\left[E_n(1-\alpha_n^*)e^{ik_n^* h_n} + F_n(1+\alpha_n^*)e^{-ik_n^* h_n}\right] \tag{3}$$

In which h_n and ρ_n are thickness and density, k_n^* is the complex wave number defined by $k_n^* = \omega / v_n^*$, v_n^* and α_n are the complex shear wave velocity and impedance ratio ($\alpha_n = \rho_n v_n^* / \rho_{n+1} v_{n+1}^*$) of n^{th} soil layer respectively. At the ground surface

$$\tau = \rho d \frac{\partial^2 u}{\partial t^2} \tag{4}$$

which governs the equality of

$$\frac{F_1}{E_1} = \frac{i + d.k_1^*}{i - d.k_1^*} \tag{5}$$

In the above relation, d is the height of surcharge mass which is equated to height of a virtual soil layer with characteristics of first layer. Using a recursive iteration scheme and adopting Eqs. (2) and (3) and (5), we calculate E_2 and F_2 in terms of E_1 and then E_3, F_4 in terms of E_2 and so forth... This iteration procedure is continued until E_{m+1}, F_{m+1} are finally calculated. Since all values of E_{m+1} and F_{m+1} are known, the displacement, stresses and strain are defined at any level of the soil stratum as a function of frequency ω of input motion. The amplification functions for elastic bedrock are denoted by A_n (ω) and is given by

$$A_n = \frac{u_n}{u_{n+1}} = \frac{E_n}{E_{n+1}} \tag{6}$$

Step 3: At this stage, the bedrock displacement $u_{m+1}(\omega)$ is multiplied by $A_m(\omega)$ which is the

amplification function for the m^{th} layer. This results in the displacement at the surface of m^{th} layer known as $u_m(\omega)$. This process is repeated until the displacement at the surface of first layer $u_1(\omega)$ is obtained. Next, the displacements in time domain at any depth in soil layers and also at any interface between two adjacent layers, is obtained using IFFT procedure, i.e.

$$u_n(\omega) = A_n(\omega) \times u_{n+1}(\omega), \qquad 1 \le n \le m \tag{7}$$

$$u_n(t) = IFFT(u_n(\omega)) = \frac{1}{N}\sum_{t=1}^{N} u_n(\omega) w_N^{-(\omega-1)(t-1)}, \qquad w_N = e^{-2\pi i/N} \tag{8}$$

Step 4: The shear strain at the middle of any given layer can be calculated as

$$\gamma_n(t) = \frac{u_n(t) - u_{n+1}(t)}{h_n} \tag{9}$$

Step 5: In nonlinear analysis which follows hereafter, shear modulus varies depending on the level of shear strain. Hence, iterative procedure is adopted such that shear modulus becomes compatible with corresponding shear strain. Convergence is usually reached when pseudo values are vanished. Possibility of divergence is, in fact, very low since iteration procedure is properly conducted throughout the course of calculations.

The shear modulus and damping ratio of the soil layers as well as the bedrock are updated using the shear strains obtained above and based on the soil's stress-strain curves similar to those shown in Figs. 1 and 2. The curves in these figures have been proposed for sandy soil and clay by Seed and Idriss (1970). These figures present rather mild nonlinearity of material (soil) since slope of the curves are not steep. However, in sever nonlinearity, presented by drastic dipping curves, results obtained from linear and nonlinear analysis differ significantly. This is because such sharply sloping curves induce drastic change in G values over a smaller range of shear strain variations.

Step 6: Considering the progressive Newton-Raphson procedure and the regular iteration used for nonlinear analysis, the pseudo-linear displacements are calculated as

$$\Delta u_{n,i}(t) = \frac{G_{n,i-1} - G_{n,i}}{G_{n,i-1}} \gamma_{n,i}(t) \times h_{n,i} \tag{10}$$

In which $G_{n,i}$,$\gamma_{n,i}$ and $\Delta_{n,i}$ are the shear modulus, shear strain and pseudo linear displacements at n^{th} layer and in i^{th} iteration respectively. In each cycle, the thickness of the layers ($h_{n,i}$) is assumed to remain constant.

Step 7: $\Delta_{n,i}$ is considered as the new input which is applied to the bedrock and response is calculated at the surface. The steps 1 to 7 above are repeated until the amplitude of $\gamma_{n,i}$(t) become small enough or less than a prescribed value (i.e., $\gamma_{n,i}(t) \le error$).

Step 8: Collective response at the surface of the layered soil system in all iterations is obtained, using the following relation, and is considered as the total nonlinear response of the system.

$$u_{tot}(t) = u_1(t) + \sum_{i=1}^{k} \Delta u_{1,i}(t) \tag{11}$$

In which $u_{tot}(t)$ is the total displacement at the ground surface and k is the number of cycle to reach the convergence. The successive steps described above have been integrated into a regular algorithm and a computer program has then been developed in MATLAB software. The program *SURCHRESPONSE* (Saffarian 2013) receives the input data including the geometrical and mechanical properties of the soil layers and surcharge mass as well as the information on loading characteristics. The output of the program includes the surface response including acceleration, velocity and displacement in time domain and even, if required by user, the seismic response spectrum of the layered soil system.

It is of note that the program developed and discussed in this part of the paper, was in fact an extension and a complement to the program described in part I. The extension of the program deals with nonlinear analysis while the initial program, used in part I, primarily carried linear analysis. For linear analysis, program first follows up to step 3, If nonlinear analysis is requested, order is given to the program to further follow steps 4, 5, … and to proceed to final results at step 8.

3. Examples

3.1 Example 1

Nonlinear seismic response of single soil layer is investigated in this example. Soil layer includes sand deposits overlain the bedrock and their properties are summarized in Table 1. Nonlinear analysis of the problem follows Seed and Idriss (1970) fundamental curves shown in

Table 1 Geometrical and mechanical properties of layered soil in example 1

Equivalent surcharge height (m)	Bed rock			Soil			
15	V_r (m/s)	μ_r (%)	γ_r (KN/m^3)	Shear velocity V_s (m/s)	Damping ratio (μ_s (%))	γ_s (KN/m^3)	Layer height (m)
0	1400	2	24	180	5	17	20

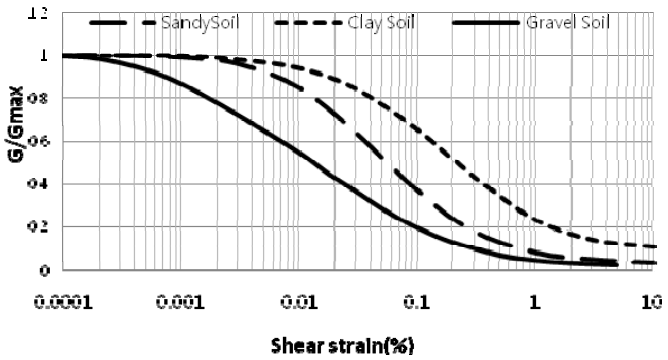

Fig. 1 Variation of shear modulus with shear strain amplitude for sand, clay and gravel soils (Seed and Idriss 1970)

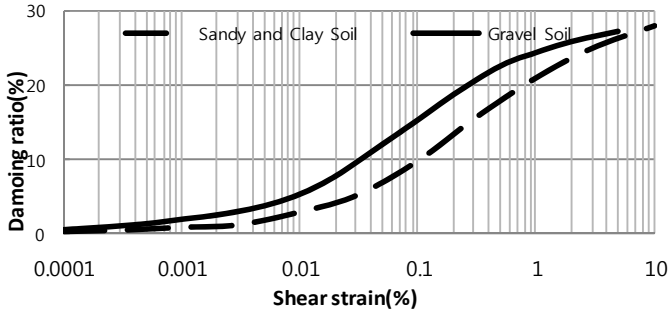

Fig. 2 Variation of damping ratio with shear strain amplitude for sand, clay and gravel soils (Seed and Idriss 1970)

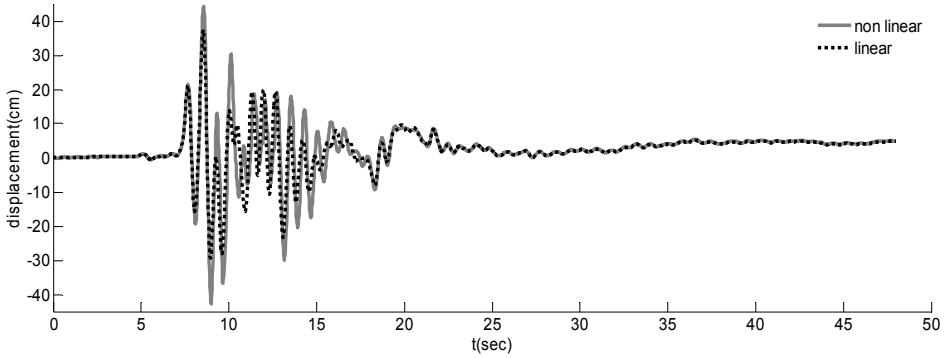

Fig. 3 Ground surface acceleration time history for Kobe (1995) earthquake calculated based on current linear and nonlinear approaches

Figs. 1 and 2. The time history of acceleration related to Kobe earthquake of 1995 is used as excitation at bedrock and as input of strong motion for the computer program developed in this study.

Results are shown in Figs. 3 to 5. Fig. 3 shows comparison of the linear and nonlinear ground surface response subjected to Kobe earthquake of 1995 record. In Fig. 4, variation of shear modulus of soil (based on curves of Fig. 1) in first cycle of iteration required for nonlinear analysis is presented. It can be seen from this figure that the shear modulus of soil varies drastically in response to the strains induced by earthquake loading. Further investigation into Fig. 4 indicates that the sharpest drop in shear modulus magnitude of soil approximately corresponds to the occurrence of peaks in acceleration time-history of earthquake. This phenomenon can be attributed to the predominant period of this earthquake record which occurs very close to the fundamental frequency (lowest natured frequency) of soil layer.

This corresponds also to the largest amplification of soil continua and, hence, results in the soil to be strained larger than the linear limit and to exhibit its nonlinear behavior.

In Fig. 5, the spectra are presented for ground surface response in two different cases related to linear and nonlinear behavior of soil. It can be seen from Fig. 5 that the assumption of nonlinear behavior of soil and application of Fig. 1 in the analysis sequence results in lower spectral

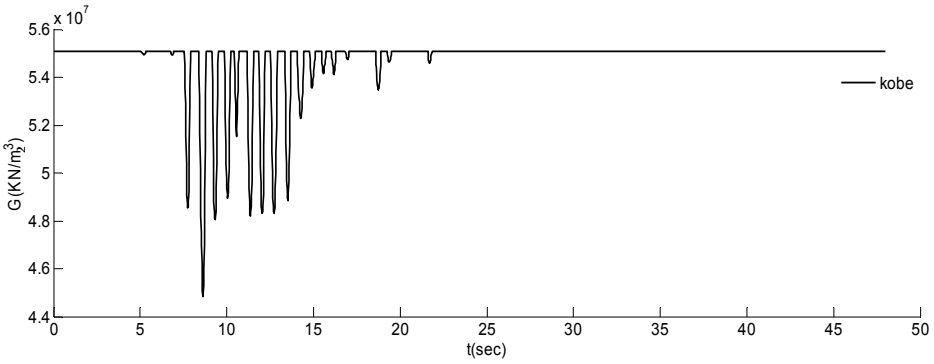

Fig. 4 Variation of shear modulus vs. time in soil layer of example 1 subjected to Kobe (1995) earthquake

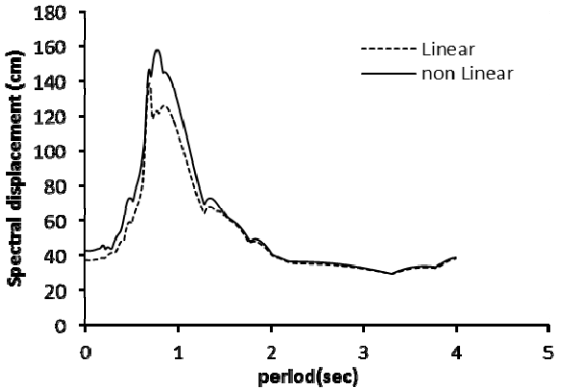

Fig. 5 Comparison of spectral displacement at ground surface using nonlinear and linear approach

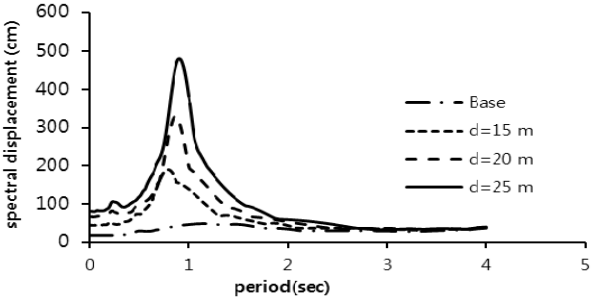

Fig. 6 Comparison of spectral displacement at bedrock and ground surface with (d =15, 20, and 25 meters) using nonlinear approach

displacements compared with that related to linear behavior of soil. In Fig. 6, the difference between the bedrock and the ground surface spectra with various height of equivalent surcharge is presented. It can be seen in this figure that displacement at ground surface is much amplified at a lower period while the lower peak in bedrock displacement is moved towards longer periods. This

again is referred to the difference between the fundamental frequencies of bedrock and of the soil layer.

3.2 Example 2

In example 2, a layered soil system studied also by Nimtaj (2010) underlining a surcharge mass is investigated. Fig. 7 presents the variation of geometrical and mechanical properties of the soil layers as well as the height of the equivalent surcharge adopted for this investigation.

Figs. 8(a) to (c) schematically shows variation of shear wave velocity, density and maximum shear modulus of soil with depth. It can be seen that the shear wave velocity and maximum (initial) shear modulus of soil generally increase with increase in depth. Such a general trend in density of soil encounters a sudden reversal at depth of -20 m, perhaps because of the presence of underground water lable. Following degradation curves (also known as fundamental curves) presented in Figs. 1 and 2 for variation of G/G_{max} and damping ratio, the effect of presence of surcharge mass on the ground surface is studied. "Degradation curves" shown in Fig. 1, was in fact the reduction of shear modulus with increase in shear strain. Degradation is also reflected through damping curves shown in Fig. 2 as when shear strain increases, damping is directly increases. Both Figs. 1 and 2 depict effect of softening of material as increasing number of loading cycles cause accumulation of strains.

Seismic displacement spectrum for layered soil system is developed assuming also nonlinear behavior of soil using fundamental curves of Figs 1 and 2. It has been observed that the lowest soil

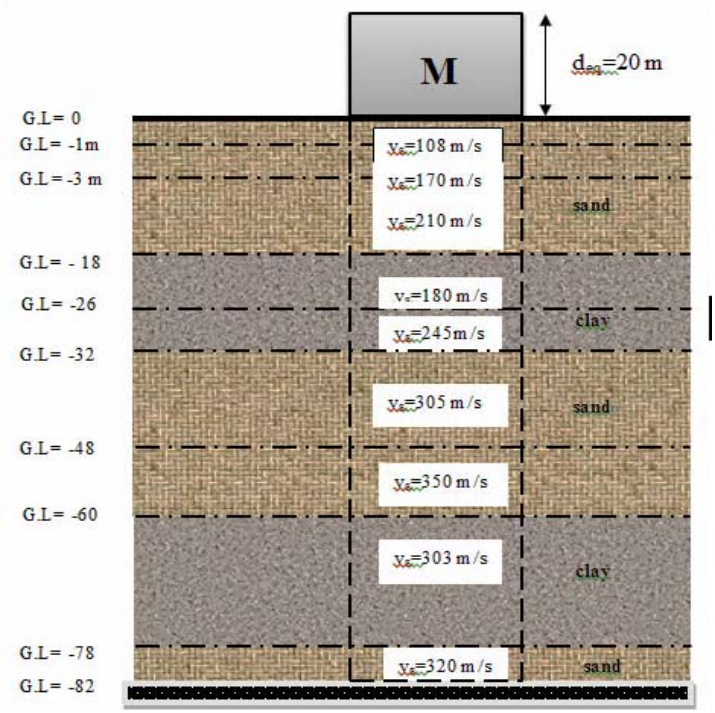

Fig. 7 Soil profile in example

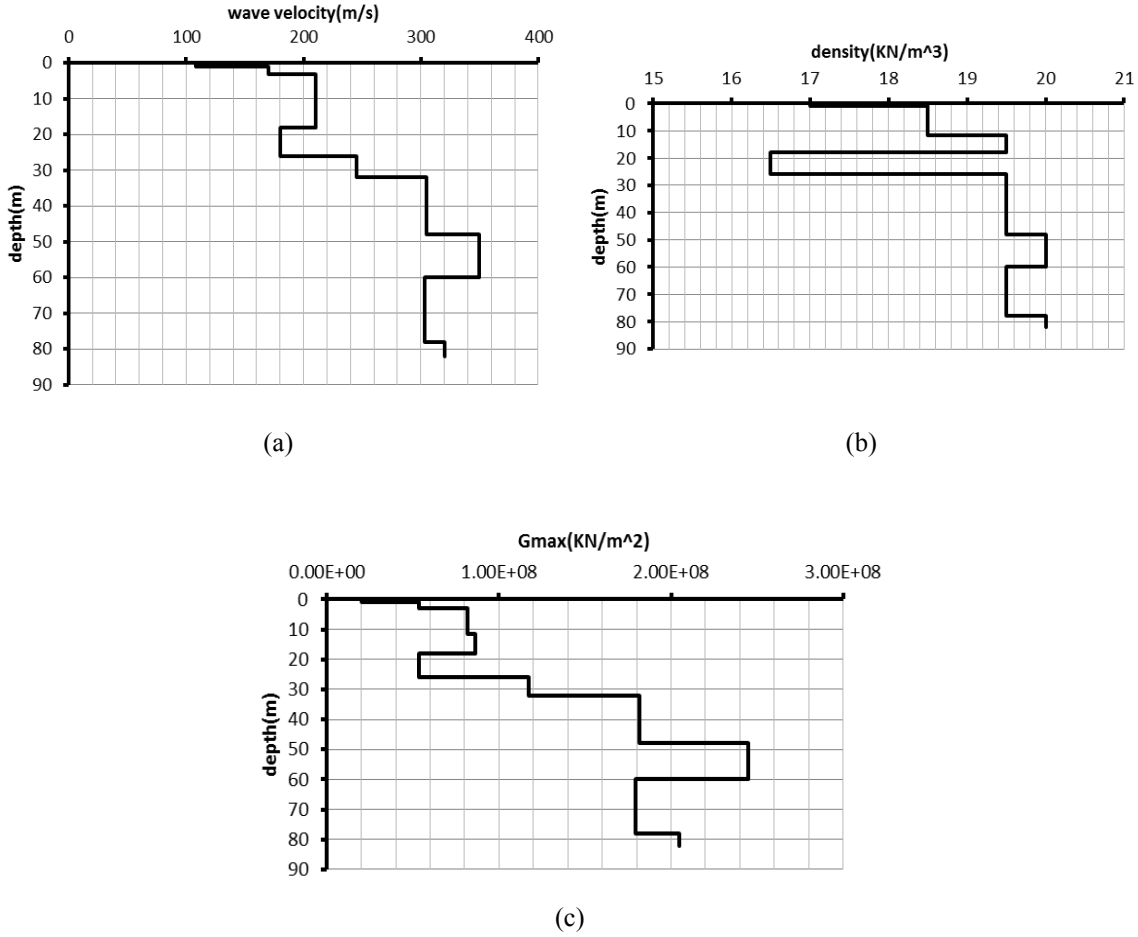

Fig. 8 Variation of: (a) Shear wave velocity; (b) Density; (c) Initial shear modulus with depth in (Nimtaj 2010)

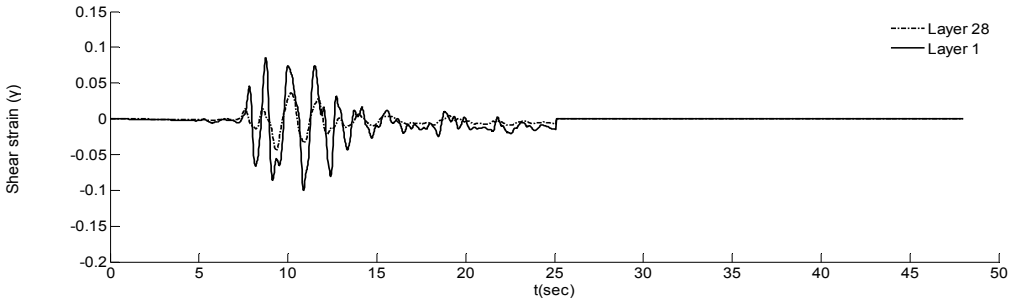

Fig. 9 Variation of shear strains induced to top and bottom layers (layers 1 and 28) during 1st cycle of cycle of nonlinear analysis

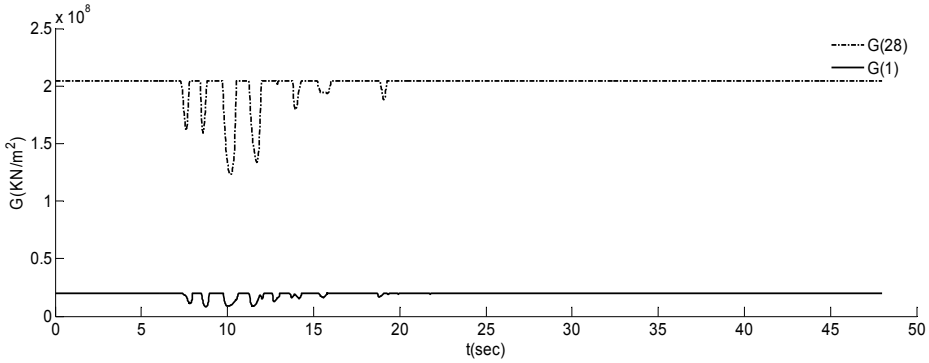

Fig. 10 Variation of shear modulus vs. time in top and bottom layers (layers 1 and 28) developed during 1st cycle of nonlinear analysis investigated in example 2

layer (bottom layer) presents the most significant difference with the top layer. Therefore, in Fig. 9, the time histories of shear strain developed at top and at bottom layers are shown. The figure shows, in fact, variation of shear strains with time developed in first cycle of the nonlinear analysis.

Fig. 10 also presents variation of shear modulus with time in the same cycle. Fundamental curves shown in Figs. 1 and 2 are used to calculate the variation of shear modulus corresponding to variation of shear strain developed in soil layers.

Fig. 10 also presents variation of shear modulus with time in the same cycle. Fundamental curves shown in Figs. 1 and 2 are used to calculate the variation of shear modulus corresponding to variation of shear strain developed in soil layers. For example, such calculations are carried (according to step 5 of the step-by-step procedure described before for nonlinear HFTD analysis approach) for bottom and top layers and results are graphically shown in Fig. 10.

Nonlinear analysis based on the HFTD method developed in this study requires calculation of the pseudo – displacements due to nonlinear behavior of soil in each cycle of iteration procedure described in previous section and for each individual layer of soil profile. These displacements, in fact, are updated in each cycle and new values are obtained. The process is continued for some consecutive cycles until convergence is reached for the shear modulus to its corresponding shear strain. The process corresponds to step 6 of the step-by- step procedure described earlier in this paper.

Further, Fig. 11 shows pseudo-displacements developed at bases of layers 1 and 28 due to earthquake loading and at first cycle of nonlinear analysis while Fig. 12 presents the corresponding transferred displacement at surface of the same layers. In surface of top layer, five iterations sufficed to conclude the convergence of procedure. The displacement time-history of the layer is shown, after convergence in nonlinear analysis is reached, in Fig. 13 associated with the results obtained for linear analysis. It can be seen from the figure that the displacements obtained in linear and nonlinear analysis are almost the same in much of time-span of displacement response except in a local time span which approximately corresponds to occurrence of peak in the acceleration time- history where PGA is observed.

Further investigation was carried into study the effect of the surcharge geometry on the displacements induced on the soil layers.

Fig. 14 depicts the variation of displacements calculated in depth of the layered soil system and for three different adopted heights of surcharge mass. It can be seen that increase in equivalent height of surcharge leads to increase in the displacements at surface of each layer especially at the top one. Such gaps depend not only on the properties of surcharge, but also on the characteristics of the soil underneath and stress field. The figure clearly shows the gaps are reduced at greater depths due to increase in effective stress. At lower depths, especially at the surface, smaller stresses on the soil cause wider gaps.

Spectral displacements calculated for ground surface and bedrock motion induced by Kobe earthquake of 1995 are shown in Fig. 15. It is deduced from this figure that seismic amplification is seen in spectral displacements with various height of surcharge. Further comparison between the seismic linear and nonlinear behavior of soil is carried using spectral displacements. Such a comparison is provided in Fig. 16 where the spectral displacements for ground surface obtained for Kobe earthquake of 1995 and for linear and nonlinear HFTD approach are shown. The little difference observed between the results of linear and nonlinear HFTD is referred to the interaction of surcharge mass at the surface. In fact, the surcharge contains the response in both linear and nonlinear approaches.

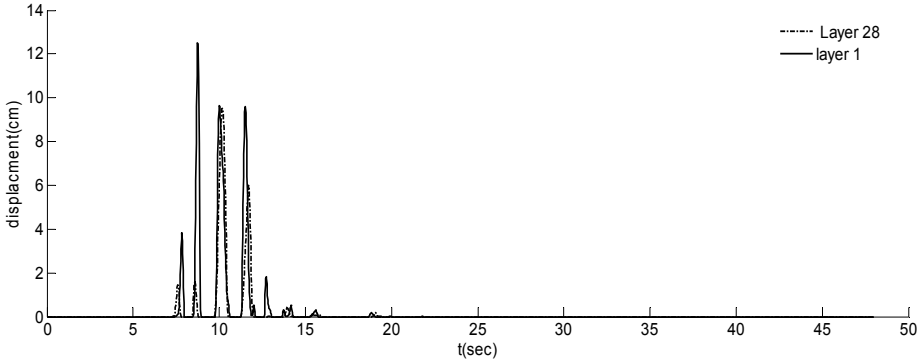

Fig. 11 Pseudo displacement vs. time calculated in nonlinear analysis at bases of layers 1 and 28 as input motion during 1st cycle of nonlinear analysis

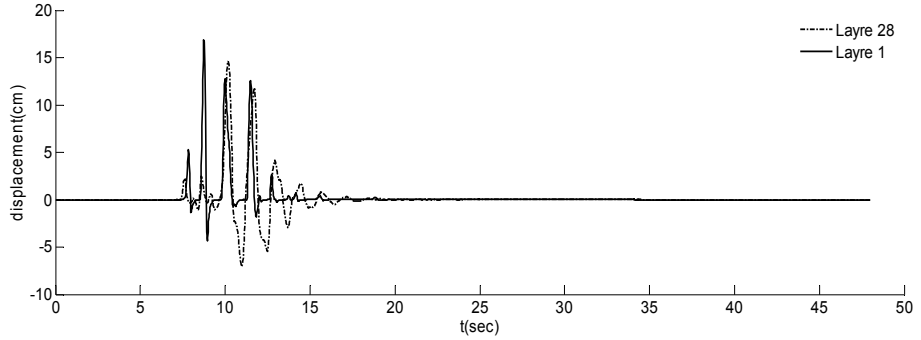

Fig. 12 Pseudo displacements calculated at the surfaces of layers 1 and 28 developed during 1st cycle of nonlinear analysis

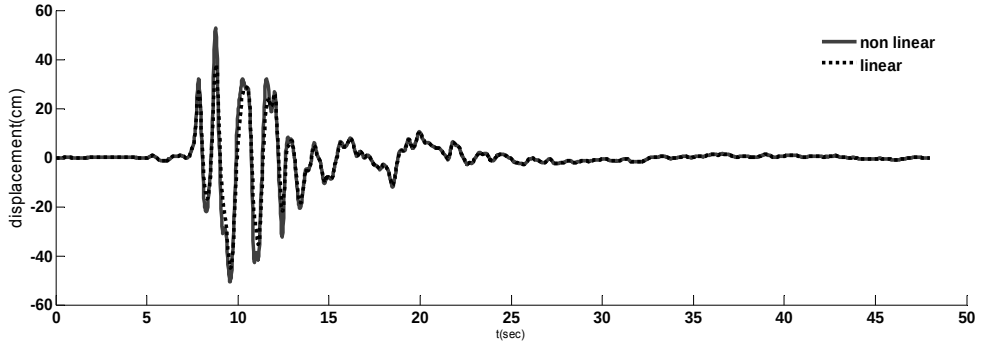

Fig. 13 Comparison of linear ground surface response with that obtained at 5th cycle of nonlinear analysis led to convergence

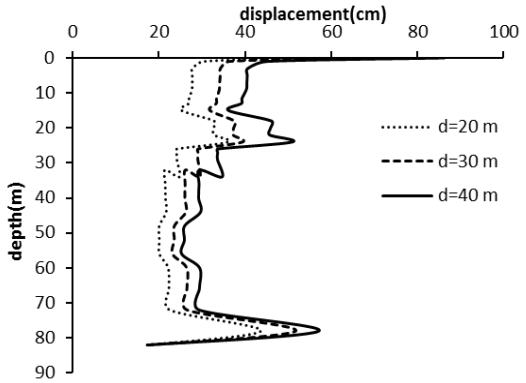

Fig. 14 Variation maximum displacement vs. depth for 3 different equivalent surcharge heights

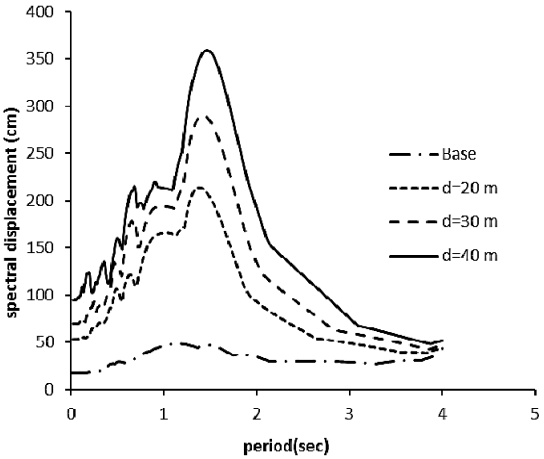

Fig. 15 Comparison of bedrock spectral displacements and nonlinear spectra for ground surface having 3 different equivalent surcharge heights (μ = 5%)

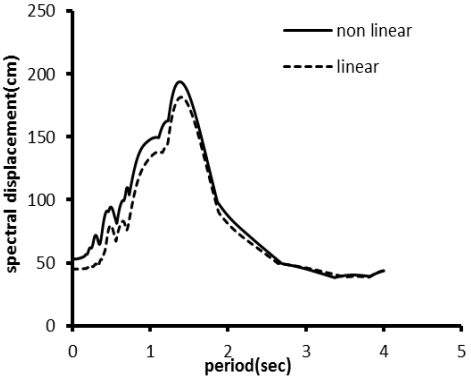

Fig. 16 Comparison of linear and nonlinear spectral displacement calculated for ground surface in example 2 (μ = 5%)

4. Conclusions

In this part of paper, effect of surcharge mass on nonlinear seismic response of a surcharged layered soil was investigated. Computer program developed for linear analysis was extended for nonlinear analysis. Despite linear analysis, fundamental curves governing the changes in shear modulus and damping in term of shear strain is defined prior to nonlinear analysis. Such curves allows the extended computer program to follow these fundamental curves and to converge to the final state where shear modulus corresponds to shear strains induced to the individual soil layers during seismic motion. Progressive Newton-Raphson method used in the development of the current approach has relatively more efficiency than classic Newton-Raphson method. Computer program was developed which, when properly run and necessary parameters are given, automatically calculates and depicts the results.

In soils with medium relative density, HFTD method works similar to linear concepts since the level of strain are sufficiently low. Further, if maximum Fourier amplitude occurs at low frequency, significant increase in surface displacement develops. Various parameters affect results of seismic analysis of soil layers including; equivalent height of surcharge, impedance ratio of adjacent layers, damping of soil layers and bedrock as well as density of individual soil layers.

References

Anbazhagan, P., Aditya, P. and Rashmi, H.N. (2011), "Amplification based on shear wave velocity for seismic zonation: Comparison of empirical relation and site response results shallow engineering bedrock sites", *Geomech*. *Eng*., *Int*. *J*., **3**(3), 189-206.

Asgari, A. and Bagheripour, M.H. (2010), "Earthquake response analysis of soil layers using HFTD approach", *Proceedings of the Geoshanghai International Conference on Soil Dynamic and Earthquake Engineering*, *ASCE Geotechnical Special Publication No. GSP 201*, Shanghai, June.

Bazrafshan Moghaddam, A. and Bagheripour, M.H. (2012a), "Ground response analysis using non-recursive matrix implementation of hybrid frequency-time domain (HFTD) approach", *Scientia Iranica*, **18**(6), 1188-1197.

Bazrafshan Moghaddam, A. and Bagheripour, M.H. (2012b), "Earthquake time – frequency analysis using a new compatible wavelet function family", *Earthq. Struct., Int. J.*, **3**(6), 839-852.

Darber, G.R. and Wolf, J.P. (1988), "Criterion of stability and implementation issues of hybrid frequency-time domain procedure for non-linear dynamic analysis", *Earthq. Eng. Struct. Dyn.*, **16**(4), 569-581.

Giarlelis, C., Lekka, D., Mylonakis, G. and Karabalis, D.L. (2011), "Lefkada 2003, Greece, earthquake: dynamic response of a 3-storey R/C structure on soft soil", *Earthq. Struct., Int. J.*, **2**(3), 257-277.

Jayaram, N., Baker, J.W., Okano, H., Ishida, H., McCann, M.W. and Mihara, Y. (2011), "Correlation of response spectral values in Japanese ground motions", *Earthq. Struct., Int. J.*, **2**(4), 357-376.

Nimtaj, A. (2010), "Seismic response of soil layers by mass -spring -damper model using Hybrid Frequency-Time Domain (HFTD) method", M.Sc. Dissertation, Shahid Bahonar University of Kerman, Kerman, Iran.

Roy, N. and Sahu, R.B. (2012), "Site specific ground motion simulation and seismic response analysis for microzonation of Kolkata", *Geomech. Eng., Int. J.*, **4**(1), 1-18.

Saffarian, M.A. (2013), "Seismic nonlinear ground response analysis considering surcharge mass by HFTD method", M.Sc. Dissertation, Shahid Bahonar University of Kerman, Kerman, Iran.

Seed, H.B. and Idriss, I.M. (1970), "Soil moduli and damping factors for the dynamic response analysis", *Report No. EERC 70–10*, *Earthquake Engineering Research Centre*, University of California, Berkeley, CA, USA.

Wolf, J.P. (1986), "Nonlinear soil-structure-interaction analysis based on hybrid frequency time domain formulation", *Proceedings of the 8th European Conference on Earthquake Engineering*, Lisbon, Portugal, September.

Zerva, A., Morikawa, H. and Sawada, S. (2012), "Criteria for processing response-spectrum-compatible seismic acceleration simulated via spectral representation", *Earthq. Struct., Int. J.*, **3**(3), 341-363.

CC